Sterilization Matters: Consequences of Different Sterilization Techniques on Gold Nanoparticles

*Á*ngela França, Beatriz Pelaz, María Moros, Christian Sánchez-Espinel, Andrea Hernández, Cristina Fernández-López, Valeria Grazú, Jesús M. de la Fuente, Isabel Pastoriza-Santos, Luis M. Liz-Marzán, and África González-Fernández*

Nanoparticles (NPs) can offer many advantages over traditional drug design and delivery, as well as toward medical diagnostics. As with any medical device or pharmaceutical drug intended to be used for in vivo biomedical applications, NPs must be sterile. However, very little is known regarding the effect of sterilization methods on the intrinsic properties and stability of NPs. Herein a detailed analysis of physicochemical properties of two types of AuNPs upon sterilization by means of five different techniques is reported. In addition, cell viability and production of reactive oxygen species are studied. The results indicate that sterilization by ethylene oxide seems to be the most appropriate technique for both types of NPs. It is concluded that it is crucial to test several methods in order to establish the specific type of sterilization to be performed for each particular NP.

Keywords:
- cytotoxicity
- gold nanoparticles
- nanoparticle stability
- reactive oxygen species
- sterilization techniques

1. Introduction

Nanoparticles (NPs) are a relatively new class of biomedical products. Their potential use in medical devices or as drug-carrier systems offers opportunities for novel therapy of complex disorders such as cancer and inflammatory and neurodegenerative diseases.[1–5] NPs based on Au chemistry have attracted significant research and practical attention. AuNPs are versatile agents with a large potential in biomedical applications, such as tumor thermal ablation, contrast agents, phototherapy, and radiotherapy enhancement treatments, as well as in drug and gene delivery.[4–11]

Chemical functionalization strategies to improve the solubility and stability of NPs have also been the subject of intense activity.[12–14] Several methodologies have been applied toward this goal. The most stable AuNPs are provided by the chemisorption of thiolated molecules onto the NP surface. One of the most efficient coating agents is the non-natural amino acid tiopronin. Tiopronin can provide interesting properties to AuNPs because it has a free terminal $-CO_2H$ group that not only imparts solubility to NPs in physiological conditions, but also a better handle for further reactivity.[15] Another interesting coating is poly(ethylene glycol) (PEG). When this hydrophilic polymer is adsorbed onto the NPs, surface hydration is largely enhanced, thus providing solubility and in vivo compatibility of the particles.[1,16,17]

The versatility of AuNPs and the potential variety of coatings render these NPs very attractive in the biomedical field. However, AuNPs still present considerable challenges before their actual use in vivo. As with any device or pharmaceutical drug, NPs intended for in vivo biomedical applications must be tested for sterility. Any contamination might invalidate subsequent studies and induce toxicity and/or

Prof. Á. González-Fernández, Á. França, C. Sánchez-Espinel, A. Hernández
Immunology Area and Unidad Compartida Complejo Hospitalario Universitario de Vigo
Edificio Ciencias Experimentales
University of Vigo
Campus As Lagoas-Marcosende
36310 Vigo (Spain)
E-mail: africa@uvigo.es

Dr. J. M. de la Fuente, Dr. V. Grazú, B. Pelaz, M. Moros
Biofunctional Nanoparticles and Surfaces Group
Aragon Nanoscience Institute (INA)
University of Zaragoza
Pedro Cerbuna 12, 50009 Zaragoza (Spain)

Prof. L. M. Liz-Marzán, Dr. I. Pastoriza-Santos, C. Fernández-Lo´pez Departamento de Química Física and Unidad Asociada CSIC University of Vigo
36310 Vigo (Spain)

infectious diseases.[18] The complete destruction of all living organisms, including bacterial spores and viruses, is achieved through sterilization. Several sterilization methods can be used, including physical methods such as autoclaving and UV irradiation, which comprise moist heat and dry heat, respectively, and chemical treatment such as using hydrogen peroxide gas plasma, ethylene oxide, and chemical vapor, which include both gaseous and liquid solutions. Nevertheless, little is known about the effects that sterilization can induce on NPs[19–21] and on their coatings. There is wide evidence that the physicochemical properties, such as size and surface chemistry, can dramatically affect the behavior of NPs in biological systems[22–25] and might, in part, determine the biodistribution, safety, and efficacy of the particles.[18] Sterilization remains a critical step for the in vivo use of NPs, and the effects of sterilization on the integrity of the physicochemical properties of NPs needs to be investigated. In this paper, we describe the effects of five types of sterilization methodologies: UV irradiation (UV), autoclaving (auto), ethylene oxide treatment (EtO), formaldehyde treatment (FM), and gas plasma treatment (GP) on AuNPs with two different sizes and surface coatings, 2-nm Au@tiopronin and 60-nm Au@PEG.

2. Results and Discussion

The use of AuNPs for optical diagnostics or medical treatments requires their prior sterilization, but the process can affect their intrinsic properties. Herein, the influence of the most commonly used sterilization techniques on the physical properties of Au colloids is analyzed. As models, Au nanocrystals of two well-differentiated sizes (2 nm and 60 nm), both highly stable in physiological media, were chosen. The 2- and 60-nm nanocrystals were protected with tiopronin and thiolated-PEG (SH-PEG), respectively. Changes in the particle morphology and stability after sterilization were studied by transmission electron microscopy (TEM) and UV–Vis spectroscopy (AuNPs present size-dependent optical properties in the visible region, and a change in the absorbance band would indicate changes in particle size or NP aggregation). Since the capping agent is responsible for the stability of metal NPs, the aggregation or particle evolution might be a result of the degradation of the protecting layer around the particles during sterilization. Thermogravimetric analysis (TGA) and/or Fourier transform infrared (FTIR) spectroscopy techniques were used to analyze the effect of sterilization on either tiopronin or PEG layers.

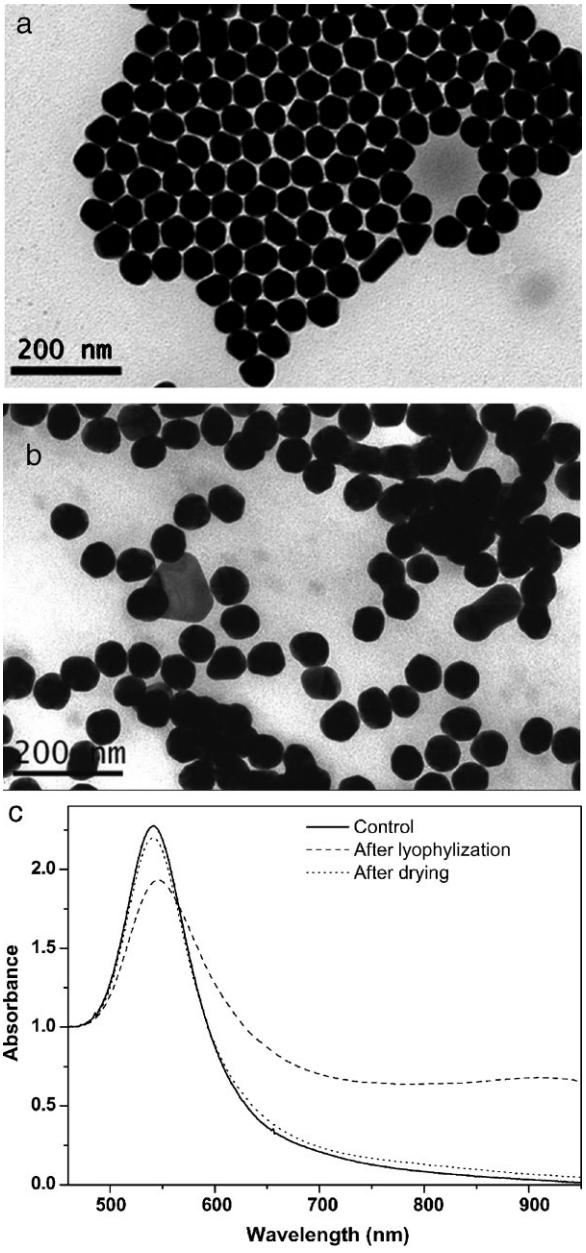

Figure 1. TEM images of Au@PEG NPs before (a) and after (b) lyophilization. UV–Vis spectra (c) of Au@PEG NPs in PBS solution of control (solid line), after lyophilization (dashed line), and after drying (dotted line).

2.1. Lyophilization of NPs

Some sterilization methods, such as gas plasma, require the use of dry NPs, since humidity could lead to breakage of the sterilization cycle. AuNPs were dried out by lyophilization and their intrinsic properties were then analyzed. Our results indicate that while the stability of Au@tiopronin NPs does not change during the lyophilization process (data not shown), the Au@PEG stability is altered (Figure 1). TEM images showed that lyophilization promotes the coalescence of some Au@PEG NPs into large aggregates with irregular shapes (Figure 1b).

It is well-known that the UV–Vis spectra of aqueous AuNP solutions depend strongly on particle size, shape, and aggregation state.[26,27]

As expected for an aggregated sample, the UV–Vis spectrum of Au@PEG after lyophilization showed a less intense surface plasmon resonance (SPR) band, which was broader and red-shifted as compared with that from the control (Figure 1c). Additionally, the presence of aggregates also produces the observed increase of absorbance at higher wavelengths. Oppositely, Au@tiopronin NPs are protected by a tightly packed and well ordered monolayer due to strong hydrogen bonding between adjacent tiopronin molecules. This

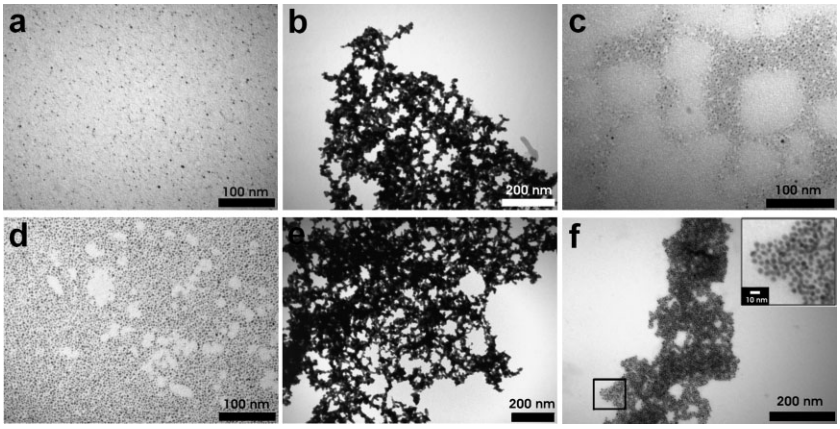

Figure 2. Representative TEM images showing the effect of different sterilization procedures on the morphology and size distribution of Au@tiopronin nanoparticles: a) control, b) UV irradiation, c) gas-plasma treatment, d) ethylene oxide treatment, e) formaldehyde treatment, and f) autoclaving.

could be the reason why these NPs can be repeatedly isolated and redissolved with no changes in their optical properties.[28] In the case of Au@PEG NPs, PEG coating was achieved by place-exchange reaction in water using a SH-PEG molecule. Most likely due to the random coil molecular conformation of PEG molecules in aqueous solution,[29–31] the PEG shell is not as tight as that formed by tiopronin. Some NP surface areas with a lower density of PEG chains could become exposed during dehydration by lyophilization due to conformational changes of the grafted PEG molecules. This could be a likely explanation of the observed (partial) aggregation. We therefore conclude that lyophilization is not a suitable method to obtain dry Au@PEG NPs and thus, the Au@PEG NPs were dried at 72 °C for 24 h, approximately. Under these drying conditions the optical properties remained unaltered as evidenced from UV–Vis spectra where almost no changes were observed after drying (Figure 1c).

2.2. Sterilization of Au@tiopronin NPs

Upon sterilization of Au@tiopronin NPs by several methods, TEM analysis was performed. TEM images (Figure 2) indicated that only sterilization by gas plasma and ethylene oxide did not affect the morphology and particle size distribution (Figure 2c and d). UV and formaldehyde sterilization caused not only NP aggregation but also coalescence into larger, irregularly shaped particles (Figure 2b and e). It must be stressed that all NP samples were prepared in the same way for TEM analysis. The observed agglomeration upon UV, formaldehyde, or autoclave treatments must thus be caused by the sterilization treatment and not during TEM sample preparation.

Interestingly, autoclave sterilization promoted NP growth, as indicated by monodisperse NPs observed in the TEM images that were slightly bigger (ca. 5 nm) (Figure 2f) than the original NPs (ca. 2 nm) (Figure 2a). This is likely due to growth and recrystallization processes (known as Ostwald ripening) induced by the high temperatures used during the autoclave treatment.[32] As expected, this gave rise to a color change from brown into reddish and the appearance of a detectable SPR band (Figure 3). The UV–Vis spectra of Au@tiopronin NPs that were either not submitted to any sterilization process (control) (Figure 3) or sterilized by gas plasma and ethylene oxide (data not shown), showed an almost non-detectable SPR band as a consequence of the small particle size.[28] A similar situation was found in UV- and formaldehyde-treated NPs. Formaldehyde and UV irradiation procedures induced a different kind of aggregation to the one induced by autoclave (Figure 2b and e). We propose that in both cases the absence of SPR band variation may be related to either absorption of these aggregates at a different wavelength range due to the coalescence and irregular shape of the resulting aggregates or to aggregate sedimentation prior to the measurement.

It has been reported that alkanethiolate monolayer-protected Au clusters can be thermally decomposed by loss of the capping monolayer as (primarily) volatile disulfides, leaving an elemental Au residue.[28] Therefore, TGA could be a convenient technique to evaluate whether the different sterilization procedures affect the organic weight fraction. The thermal decomposition of all nanoparticles subjected or not to sterilization occurred in individual, well-defined steps that start at ≈230 °C and are completed after a further temperature increase of ≈100 °C. The organic fraction was nearly 35% of the total weight in all cases (Figure 4a). Additionally, no differences could be found when comparing the FTIR spectra of NPs before and after treatment with the different sterilizing procedures. The main characteristic vibrations of tiopronin as capping material, such as the N–H bending and C=O stretching modes, appear around 1400–1600 cm^{-1} in all cases (Figure 4b). Therefore, data obtained by TGA and FTIR spectroscopy indicate that the different sterilization procedures neither lead to loss of organic weight fraction nor

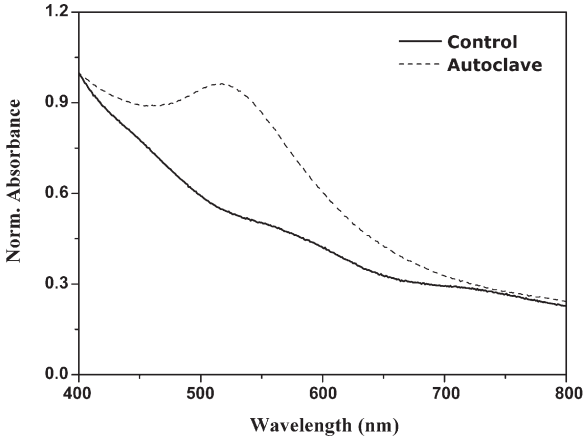

Figure 3. UV–Vis spectra of Au@tiopronin NPs before (control) and after autoclave sterilization. NPs submitted to the other sterilization procedures did not show any difference at the measured wavelengths (data not shown).

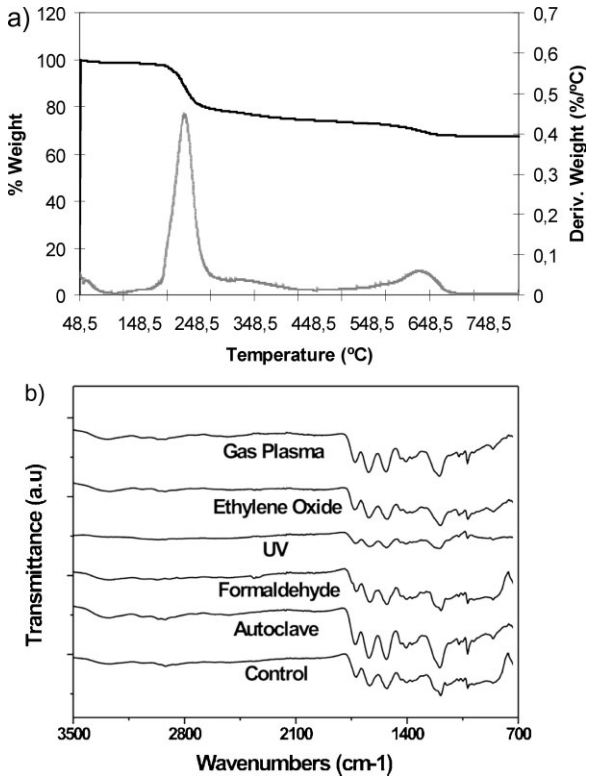

Figure 4. TGA (a) and FTIR spectra (b) of Au@tiopronin NPs. In the case of the TGA study, the black line expresses wt% and the gray line shows the TGA weight loss derivative for control Au@tiopronin NPs. NPs submitted to the other sterilization procedures did not show any difference (data not shown).

affect the intercluster hydrogen bonding between adjacent tiopronin molecules.

2.3. Sterilization of Au@PEG NPs

After the different sterilization methods, a change in solution color from red to grey was only observed in the Au@PEG dispersion sterilized by gas plasma (data not shown). This observation was in agreement with the UV–Vis spectra (Figure 5), where the gas-plasma-treated NPs present a wide absorption band along the whole visible range and even the near-IR region as a result of particle aggregation. Regarding formaldehyde and autoclave sterilization procedures, SPR bands were observed to be very similar to that of the control, although with a slightly lower intensity and a shoulder at longer wavelengths, indicating that there is a small fraction of aggregated particles. However, in the case of NPs under UV irradiation and ethylene oxide treatment, no differences were found when compared to the control. This was confirmed by TEM. As can be seen in Figure 6, gas plasma

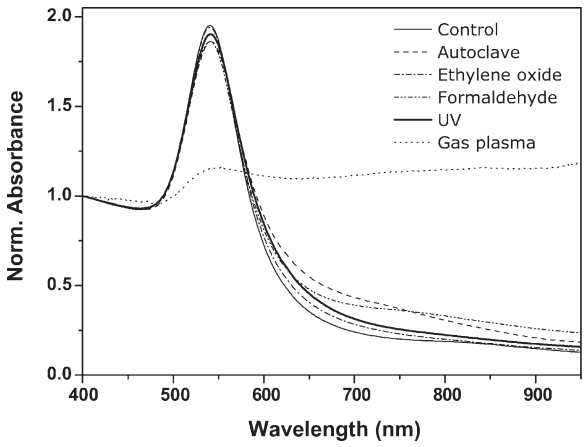

Figure 5. UV–Vis spectra of Au@PEG NP colloids before (control) and after different sterilization techniques.

caused not only aggregation of the NPs but also coalescence into larger particles of irregular shape. However, minor coalescence was observed in the NPs after formaldehyde and autoclave treatments and no alteration was observed in the particle morphology and size after ethylene oxide and UV sterilization.

The stability of the particles in biological media is provided by the PEG layer grafted onto the AuNP surface through the thiol bonding. Therefore, any alteration/degradation of the PEG shell during the sterilization process could lead to NP aggregation or coalescence. Surface FTIR spectroscopy was performed to provide more careful insights into the stability of the PEG shell around metal cores after the different sterilization procedures. Thus, the characteristic vibrational bands of PEG, C–O symmetric stretching (1 150–1 085 cm^{-1}) and C–H stretching (2 840–3 000 cm^{-1}), which can be clearly seen in the control, were analyzed for the different sterilized particles (Figure 7). Except for the case of gas plasma, the vibrational bands for PEG remain unaltered after the different sterilization processes. The treatment with gas plasma is a highly oxidative procedure that has a direct influence on PEG chemical stability.[33] Since the particles treated with gas plasma were the only ones that were clearly affected by sterilization, to

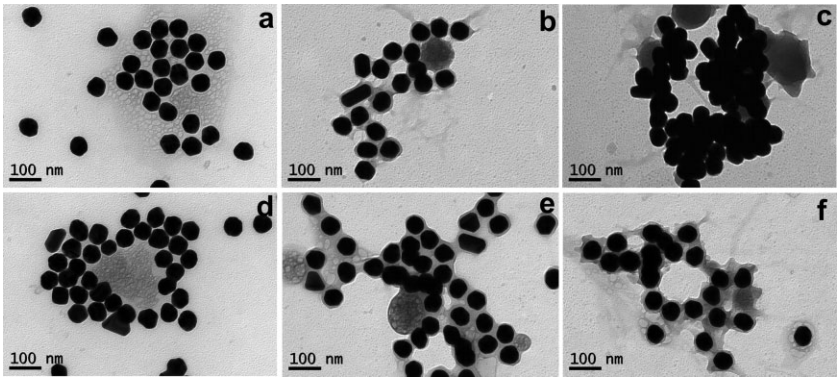

Figure 6. Representative TEM images showing the effect of the different sterilization procedures on Au@PEG NPs: a) control, b) UV irradiation, c) gas-plasma treatment, d) ethylene oxide treatment, e) formaldehyde treatment, and f) autoclaving.

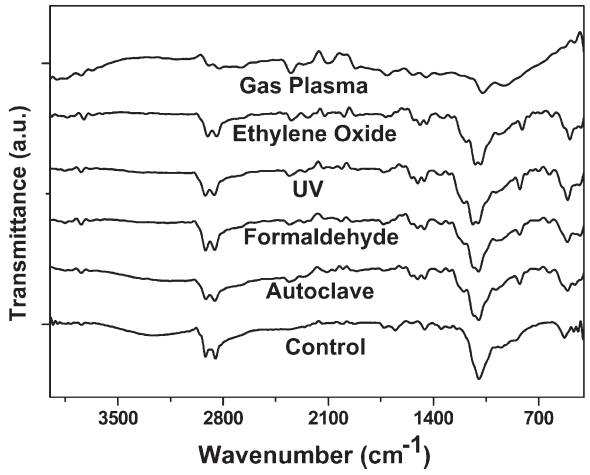

Figure 7. FTIR spectra of Au@PEG NPs before and after sterilization showing the effect of the different sterilization procedures on the external PEG layer.

some extent it seems that the stability of the NPs is given by the alteration degree of the PEG layer in such sterilized NPs.

2.4. Cytotoxicity and ROS Induction

Although non-cytotoxic effects have been widely reported for several AuNPs[34–36] and in several cells studied,[37] we evaluated the potential toxicity of sterilized NPs as well as their ability to induce reactive oxygen species (ROS)[38] in the human cell line U937 (Figure 8). Only AuNPs that did not show important alterations in their properties upon sterilization were considered for this study. Our results show that for

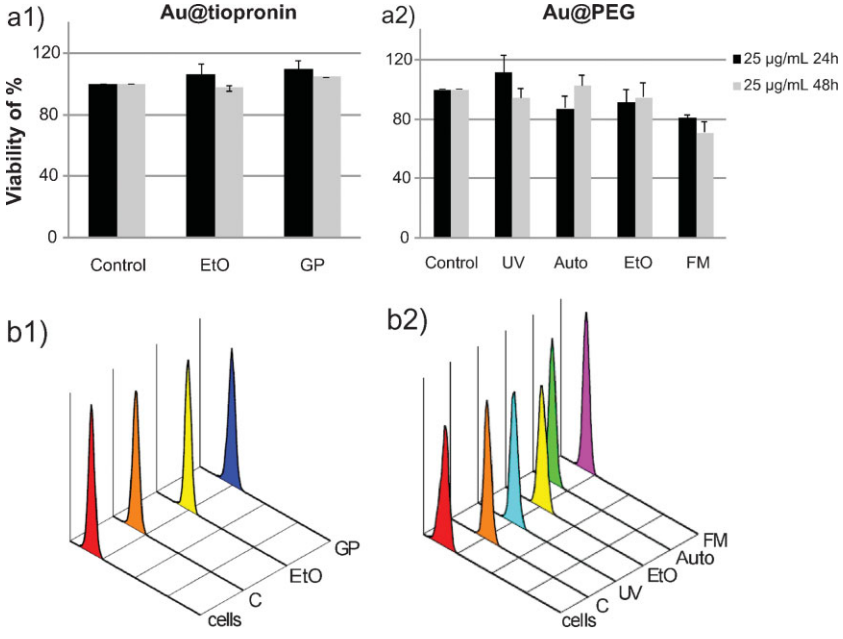

Figure 8. a) Viability of U937 cells after 24 and 48 h incubation with 25 $\mu g\,mL^{-1}$ of Au@tiopronin (a_1) or Au@PEG (b_2) NPs submitted or not to different sterilization techniques. b) ROS induction in U937 cells after 30 min with 25 $\mu g\,mL^{-1}$ of Au@tiopronin (b_1) or Au@PEG (b_2) NPs previously sterilized or not by different methods.

Table 1. General description of the physicochemical consequences of the different sterilization methods on the AuNPs (UV = UV irradiation, Auto = autoclaving, EtO = ethylene oxide treatment, FM = formaldeormaldehyde treatment, GP = gas-plasma treatment).

	Au@tiopronin				Au@PEG			
	UV–Vis	TEM	FTIR/ TGA	Viability/ ROS	UV–Vis	TEM	FTIR	Viability/ ROS
UV	√	X	√	Na	√	√	√	√/√
Auto	X	X	√	Na	±	±	√	√/√
EtO	√	√	√	√/√	√	√	√	√/√
FM	√	X	√	Na	±	±	√	X/√
GP	√	√	√	√/√	X	X	X	Na

[Na] Not analyzed. [√] Non-detectable alterations. [±] Slight alterations. [X] Strong alterations.

Au@tiopronin NPs, the sterilization processes did not affect the biocompatibility since the viability values were very similar to the control (untreated NPs) (Figure 8a_1). In the case of Au@PEG NPs (Figure 8a_2), we found a significant decrease in cell viability for NPs previously sterilized by formaldehyde (<75% of cell viability after 48 h) compared to the control. This decrease in cell viability could be related not only to the alterations observed in the NPs stability, but also to the presence of some formaldehyde residues in the NP suspension. However, other sterilization methods (UV, autoclave, and ethylene oxide) did not greatly affect cell viability.

NPs can be toxic not only by affecting the cells in a direct way, but also indirectly by the induction of ROS due to either external (membrane) or internal (after uptake) interactions with the cells. When generated in large excess, ROS can damage membrane cells and contribute to inflammation. Regarding the induction of ROS, we tested two different concentrations of NPs (0.5 and 25 $\mu g\,mL^{-1}$) and two different induction times (5 and 30 min). Figure 8b shows the results obtained using the higher concentration and longer incubation time (25 $\mu g\,mL^{-1}$ for 30 min). All sterilized NPs induced no or very low levels of intracellular ROS. In the case of Au@tiopronin (Figure 8b_1), negligible levels of ROS were induced in NPs treated with gas plasma and ethylene oxide. In the case of Au@PEG, NPs treated with UV irradiation, formaldehyde, ethylene oxide, and autoclaving induce a small amount of intracellular ROS in U937 (Figure 8b_2).

3. Conclusions

Our data indicate that careful attention should be paid when attempting to find a suitable type of sterilization method for each NP system. Additionally, it appears to be impossible to make generalizations. Despite having the same core material,

the effects of sterilization procedures on AuNPs can be totally different due to differences in the composition of organic capping agents. The procedure of choice must thus ensure sterility but also maintain the stability and physicochemical characteristics (Table 1) of NPs, such as optical properties, size, shape, absence of aggregation, surface chemistry, and biological activity. Thus, upon the sterilization procedures, several techniques (such as TEM, UV–Vis spectroscopy, FTIR spectroscopy, cytotoxicity, etc.) must be carried out to ensure that the NPs have not been affected. We show in this study that gas plasma and ethylene oxide seem to be the most appropriate sterilization methods for Au@tiopronin NPs, but gas plasma should not be used for Au@PEG NPs because it affects the PEG coating. Treatments with ethylene oxide and UV irradiation are the most suitable procedures for these NPs.

4. Experimental Section

Materials: *N*-(2-mercaptopropionyl)glycine (tiopronin)(>98%), $NaBH_4$ (98%), and O-[2-(3-mercaptopropionylamino)ethyl]-O'-methyl-polyethyleneglycol ($MW = 5000$ g mol^{-1}) were supplied by Fluka. Cellulose ester dialysis membrane (MW cut off = 10 000 g mol^{-1}), ascorbic acid, cetyltrimethylammonium bromide (CTAB), hydrogen tetrachloroaureate (III) trihydrate (99.9%) ($HAuCl_4 \cdot 3H_2O$), and trisodium citrate dihydrate were purchased from Sigma–Aldrich. In-house distilled water was further purified using a Milli-Q reagent grade water system (Millipore). Phosphate buffered saline (PBS) was purchased from Hyclone. The human cell line U937, a myelo-monocytic cell line, was supplied by ATCC (American Type Cell Culture) and fetal bovine sera (FBS) by PAA. RPMI medium (Roosevelt Park Memorial Institute) and penicillin/streptomycin were purchased from Gibco. Trypan blue and 2′,7′-dichlorofluorescein-di-acetate (DCFH-DA) were purchased from Invitrogen. Quick Cell proliferation test solution was purchased from GenScript Corporation. Buffers were prepared according to standard laboratory procedures. Other chemicals were reagent grade and used as received.

Synthesis of Au@tiopronin NPs: $HAuCl_4 \cdot 3H_2O$ (0.4 mmol) and tiopronin (1.2 mmol) were dissolved in 6:1 methanol/acetic acid (20 mL), resulting in a ruby-red solution.[15,28] An aqueous solution of $NaBH_4$ (7.5 mL, 1.07 M) was subsequently added via rapid stirring. The resulting black suspension was additionally stirred for 30 min after cooling, and the solvent removed under vacuum at 40 °C. The crude sample was insoluble in methanol but reasonably soluble in water. It was purified by dialysis, in which the pH of crude product (130 mg) dissolved in water (20 mL) was adjusted to 1 by dropwise addition of concentrated HCl. After dialysis, the dark brown Au@tiopronin solutions were lyophilized. The resulting materials were found to be spectroscopically clean and produced a yield of 96 mg of final NPs. ^{1}H NMR (400 MHz, D_2O, δ): 4.40–3.75 (m), 3.70 (bs), 2.20–1.30 (m); UV–Vis (H_2O): $\lambda = 560$ nm (surface plasmon band); IR (KBr): $\nu = 3433$, 2925, 2852, 1722, 1644, 1531, 1384, 1199, 1014, 794 cm^{-1}.

Synthesis of Au@PEG NPs: The 60-nm AuNPs were synthesized as described elsewhere.[39] Briefly, 12-nm Au seeds (0.5 mM) were prepared by citrate reduction and then diluted with the same volume of a 0.03 M CTAB solution. Seeded growth was then carried out by addition of ascorbic acid solution (5×10^{-4} M) to a mixture of $HAuCl_4$ (2.5×10^{-4} M) and CTAB (0.015 M) at 35 °C, followed by addition of the seed solution ([Au] = 4×10^{-6} M). Purification was carried out to remove rod-shaped particles.[40] For PEG-SH capping, 200 mL of the ≈60-nm Au particles was centrifuged (3000 rpm) to remove excess CTAB and redispersed in the same volume of water. Subsequently, PEG-SH (22 mL, 2 mM) was added dropwise under vigorous stirring and then allowed to react for 2 h. Finally, the sample was centrifuged to remove excess PEG-SH and redispersed in a certain amount of water.

Sterilization methods: AuNPs were divided into six aliquots of equal volume and sterilized by means of five different techniques: autoclaving, UV irradiation, ethylene oxide treatment, formaldehyde treatment, and gas plasma treatment. Autoclave sterilization was performed at 134 °C for 40 min. UV irradiation was carried out at room temperature for approximately 12 h. The ethylene oxide treatment was performed at 54 °C for 60 min. The gas-plasma procedure was carried out at 45 °C for 50 min and finally, formaldehyde sterilization was performed at 60 °C for 60 min. One aliquot was kept at 4 °C as a control for further comparison with the sterilized counterpart. Sterility was further confirmed by the absence of bacterial contamination on lysogeny broth (LB) agar plates (data not shown).

NP characterization: The analysis of the sterilized samples was carried out after the resuspension of AuNPs in PBS. Thus, UV–Vis absorbance spectra were recorded with an Agilent 8453 UV–Vis diode-array or a Shimadzu UV-3101PC spectrophotometer with a resolution of 1 nm. For TEM, a single drop (10 μL) of the different AuNP solutions was placed onto a carbon-coated copper grid and then allowed to dry in air for several hours at room temperature. TEM analysis was carried out in a JEOL JEM 1010 TEM operating at 100 kV. FTIR spectra were recorded in a Nicolet 6700 FTIR spectrometer with a resolution of 4 cm^{-1}. The data were recorded from 4000 to 750 cm^{-1}. TGA was performed using a TA STD 2960 simultaneous DTA-DTGA instrument both under inert atmosphere and in air and at a heating rate of 10 °C · min^{-1}. ^{1}H-NMR spectra of the Au@tiopronin NPs were acquired with a Bruker DRX-400 spectrometer and chemical shifts are given in ppm (δ) relative to the residual signal of the solvent used.

Cell culture: U937 cells were routinely cultured at 37 °C in a humidified atmosphere with 5% CO_2 and maintained in RPMI supplemented with 10% heat-inactivated FBS, penicillin (100 U mL^{-1}) and streptomycin (100 μL mL^{-1}). Culture media were replaced every second day. For subculture, cells were washed by centrifugation and resuspended in medium to be reseeded into a new culture flask. Routinely, cell viability during subculturing was determined by Trypan blue exclusion test.

NPs effects on cell viability: Cell viability was analyzed by Quick Cell proliferation test solution colorimetric assay. The cells were incubated in 96-well plates in the absence or presence of various concentrations of AuNPs (0.5 and 25 μg mL^{-1}) for 24 and 48 h at 37 °C and 5% CO_2. The reaction product was spectrometrically determined at 450 nm using a microplate reader (Multiskan EX, BioAnalysis Labsytems). The experiment was repeated twice and in duplicate. Results are shown as percentage of viability (%*V*) with respect to the control (untreated NPs).

ROS induction by NPs: The intracellular generation of ROS was performed with DCFH-DA to detect and quantify intracellular

production of H_2O_2. Cells were exposed to different concentra-tions of AuNPs (0.5 and 25 $\mu g\ mL^{-1}$) for 5 and 30 min and the green fluorescence of DCF was recorded with a laser excitation wavelength of 488 nm using a FACS Coulter (FC500 MPL).

Acknowledgements

We are very grateful to the Director, manager and staff from the sterilization Units of Povisa and Meixoeiro Hospitals (Complejo Hospitalario Universitario de Vigo), Vigo, Spain. We also thank the Ecology group (University of Vigo) for granting use of their lyophilization equipment. The authors acknowledge financial support from the Xunta de Galicia (PGIDIT06TMT31402PR), SUDOE (IMMUNONET-SOE1/1P1/E014), and Spanish Ministry of Science and Innovation (Consolider Ingenio 2010, CSD2006-12, NANOBIOMED). Ángela França was supported with a Leonardo da Vinci Fellowship. Jesús Martinez de la Fuente thanks ARAID for financial support. The authors declare no competing financial interest.

[1] S. E. McNeil, *J. Leukocyte Biol.* **2005**, *78*, 585.
[2] M. Ferrari, G. Dowing, *BioDrugs* **2005**, *19*, 203.
[3] M. A. Dobrovolskaia, J. Clogston, W. N. Barry, J. B. Hall, A. K. Patri, S. E. McNeil, *Nano Lett.* **2008**, *8*, 2180.
[4] S. Lal, S. E. Clare, N. J. Halas, *Acc. Chem. Res.* **2008**, *41*, 1842.
[5] R. Popovtzer, A. Agrawal, N. A. Kotov, A. Popovtzer, J. Balter, T. E. Carey, R. Kopelman, *Nano Lett.* **2008**, *8*, 4593.
[6] C. M. Goodman, C. D. McCusker, T. Yilma, V. M. Rotello, *Bioconjugate Chem.* **2004**, *15*, 897.
[7] L. R. Hirsh, R. J. Stafford, J. A. Bankson, S. R. Sershen, B. Rivera, R. E. Price, J. D. Hazle, N. J. Halas, J. L. West, *Proc. Natl. Acad. Sci. USA* **2003**, *100*, 13549.
[8] J. F. Hainfeld, D. N. Slatkin, H. M. Smiloowitz, *Phys. Med. Biol.* **2004**, *49*, 309.
[9] M. Thomas, A. M. Klibanov, *Proc. Natl. Acad. Sci. USA* **2003**, *100*, 9138.
[10] D. Shenoy, W. Fu, J. Li, C. Crasto, G. Jones, C. DiMarzio, S. Sridhar, M. Amiji, *Int. J. Nanomed.* **2006**, *1*, 51.
[11] X. H. Huang, I. H. El-Sayed, W. Qian, M. A. El-Sayed, *J. Am. Chem. Soc.* **2006**, *128*, 2115.
[12] B. C. Mei, K. Susumu, I. L. Medintz, J. B. Delehanty, T. J. Mountziaris, H. Mattoussi, *J. Mater. Chem.* **2008**, *18*, 4949.
[13] B. Dubertret, P. Skourides, D. J. Norris, V. Noireaux, A. H. Brivanlou, A. Libchaber, *Science* **2002**, *298*, 1759.
[14] W. P. Wuelfing, S. M. Gross, D. T. Miles, R. W. Murray, *J. Am. Chem. Soc.* **1998**, *120*, 12696.
[15] J. M. de la Fuente, C. C. Berry, *Bioconjugate Chem.* **2005**, *16*, 1176.
[16] T. Niidome, M. Yamagata, Y. Okamoto, Y. Akiyama, H. Takahashi, T. Kawano, Y. Katayama, Y. Niidome, *J. Controlled Release* **2006**, *114*, 343.
[17] B. Ballou, B. C. Lagergholm, L. A. Ernst, M. P. Bruchez, A. S. Waggoner, *Bioconjugate Chem.* **2004**, *15*, 79.
[18] J. B. Hall, M. A. Dobrovolskaia, A. K. Patri, S. E. McNeil, *Future Med.* **2007**, *2*, 789.
[19] B. Magenheim, S. Benita, *STP Pharma Sci.* **1991**, *1*, 221.
[20] E. Allémann, R. Gurny, E. Doelker, *Eur. J. Pharm. Biopharm.* **1993**, *39*, 173.
[21] P. Sommerfeld, U. Schroeder, B. A. Sabel, *Int. J. Pharm.* **1998**, *164*, 113.
[22] K. Ogawara, M. Yoshida, K. Higaki, T. Kimura, K. Shiraishi, M. Nishikawa, Y. Takakura, M. Hashida, *J. Controlled Release* **1999**, *59*, 15.
[23] H. Kobayashi, S. Kawamoto, S. K. Jo, H. L. Bryant, M. W. Brechbiel, R. A. Star, *Bioconjugate Chem.* **2003**, *14*, 388.
[24] K. Furumoto, S. Nagayama, K. Ogawara, Y. Takakura, M. Hashida, K. Higaki, T. Kimura, *J. Controlled Release* **2004**, *97*, 133.
[25] G. Oberdorster, E. Oberdorster, J. Oberdorster, *Environ. Health Perspect.* **2005**, *113*, 823.
[26] T. J. Norman Jr, C. D. Grant, D. Magana, J. Z. Zhang, J. Liu, D. Cao, F. Bridges, A. Van Buuren, *J. Phys. Chem. B* **2002**, *106*, 7005.
[27] L. M. Liz-Marzán, *Langmuir* **2006**, *22*, 32.
[28] A. C. Templeton, S. Chen, S. M. Gross, R. W. Murray, *Langmuir* **1999**, *15*, 66.
[29] M. Kosielsk, *J. Mol. Liq.* **2006**, *128*, 105.
[30] M. L. Alessi, A. I. Norman, S. E. Knowlton, D. L. Ho, S. C. Greer, *Macromolecules* **2005**, *38*, 9333.
[31] L. Dreesen, C. Humbert, P. Hollanber, A. A. Mani, K. Ataka, P. A. Thiry, A. Peremans, *Chem. Phys. Lett.* **2005**, *333*, 317.
[32] J. Sun, D. Ma, N. Zhang, X. Liu, X. Han, X. Bao, G. Weinberg, N. Pfänder, D. Su, *J. Am. Chem. Soc.* **2006**, *128*, 15756.
[33] J. L. Calvet, D. K. Grafaherend, M. Möller, *J. Mater. Sci.: Mater. Med.* **2008**, *19*, 1631.
[34] R. Shukla, B. Vipul, C. Minakshi, B. Atanu, R. R. Bhonde, M. Sastry, *Langmuir* **2005**, *21*, 10644.
[35] E. E. Connor, J. Mwamuka, A. Gole, C. J. Murphy, M. D. Wyatt, *Small* **2005**, *1*, 325.
[36] H. K. Patra, S. Banerjee, U. Chaudhuri, P. Lahiri, A. K. Dasgupta, *Nanomedicine* **2007**, *3*, 111.
[37] B. Díaz, C. Sánchez-Espinel, M. A. Hernández, I. Pastoriza-Santos, L. M. Liz-Marzán, Á. González-Fernández, unpublished results.
[38] B. Díaz, C. Sánchez-Espinel, M. Arruebo, J. Faro, E. de Miguel, S. Magadán, C. Yaguë, R. Fernández-Pacheco, M. R. Ibarra, J. Santamaria, A. González-Fernández, *Small* **2008**, *4*, 2025.
[39] J. Rodríguez-Fernández, J. Pérez- Juste, J. García de Abajo, L. M. Liz-Marzán, *Langmuir* **2006**, *22*, 7007.
[40] N. R. Jana, *Chem. Commun.* **2003**, 1950.

Received:
Revised:
Published online: